

***K* x-ray production in H-like Si¹³⁺, S¹⁵⁺, and Ar¹⁷⁺ ions colliding with various atom and molecule gas targets at low collision energies**

H. Tawara,¹ P. Richard,¹ U. I. Safronova² and P. C. Stancil³

¹*J. R. Macdonald Laboratory, Department of Physics, Kansas State University, Manhattan, Kansas 66506-2604*

²*Department of Physics, University of Notre Dame, Notre Dame, Indiana 46556-5601*

³*Department of Physics and Astronomy, The University of Georgia, Athens, Georgia 30602-2451*

(Received 23 April 2001; published 13 September 2001)

K x rays have been observed in electron capture processes of H-like Si¹³⁺, S¹⁵⁺, and Ar¹⁷⁺ (1*s*) ions colliding with various atom and molecule gas targets over the collision energy of 1–70 keV/*u*. These *K* x rays are the final results of cascade-down to the ground (1*s*²) state from highly excited states formed through electron capture. It has been found that at low energies (<10 keV/*u*) the cross sections for the production of *K* x rays are nearly constant, and decrease slowly when the collision energy is increased. The cross sections also have been found to increase roughly with the inverse square of the ionization energy of the targets. It is also noted that the intensity ratios of the *Kβ* line to the *Kα* line increase slightly as the ionization energy of the target increases, suggesting that an electron is captured in different (*n*′) states in different targets. These ratios are found to decrease slightly as the collision energy increases. The measured *K* x-ray production cross sections also have been compared with total electron-capture cross sections based upon an empirical formula, and it has been found that, on average, roughly two-third of total electron capture processes result in *K* x-ray emission, with the remaining one-third ending at the metastable state level after electron capture without emitting *K* x rays.

DOI: 10.1103/PhysRevA.64.042712

PACS number(s): 34.70.+e, 32.80.Rm

INTRODUCTION

In the past decades there have been reported a series of extensive experimental and theoretical investigations of the electron-capture processes involving low-energy, highly charged ions (*A*^{*q*+}) in collisions with atoms and molecules. These investigations were fueled mostly by the urgent requirement and applications to diagnostics and modeling of high-temperature fusion plasmas [1,2]. There most of the attention was paid to studying their electron-capture processes by measuring either the electron-captured (charge-changed) products including recoiled target ions or electrons or photons emitted in the collisions. To obtain a detailed understanding of the electron-capture processes and also to apply these processes to a number of different fields, not only a knowledge of “total” electron-capture cross sections is necessary but also so-called “state-selective” electron capture, namely (*nl*) distributions, is a requisite. So far little attention has been paid to x-ray emission processes involving low-energy, highly charged ion collisions, and only a few have been performed to understand the processes through x-ray observation.

It has been established that in such processes an electron of the target is captured into a highly excited (*nl*) state of the incident ion and, before it becomes stabilized, electrons, photons or x rays are emitted at various energies. The principal quantum number *n*₀ of the dominant states for electron capture into bare ions with charge *q* can be estimated through the relationship [3–5]

$$n_0 = q^{0.75} / (I_b / 13.6)^{0.5}, \quad (1)$$

where *I*_{*b*} represents the ionization energy of target species in units of eV. For example, *n*₀ = 9 for Ar¹⁷⁺ + O₂ collisions.

The electron in such a high Rydberg state [process (2) given below], instead of going down directly to the ground state via a single step [process (3) given below], tends to cascade down through a series of lower *n* states via multiple steps [process (4) given below] before finally reaching the 2*p* or 3*p* states which, in turn, emit *Kα* or *Kβ* x rays, and then get completely stabilized.

$$A^{q+} + B \rightarrow A^{(q-1)+*}(nl) + B^+ \quad (2)$$

$$\rightarrow A^{(q-1)+}(1s) \quad (3)$$

$$\rightarrow A^{(q-1)+*}(n'l') \rightarrow A^{(q-1)+*}(n''l'') \rightarrow \dots \rightarrow A^{(q-1)+}(1s). \quad (4)$$

Though the general trend indicates that, as the collision energy increase, *n*₀ becomes smaller and its distributions become broader, such a variation is expected to be relatively small over the present collision energies [2].

Most recently, since the first observation of x rays from comets, such as Hyakutake [6,7], x ray emission processes involving such highly charged ions have caused considerable attention in astrophysics applications. The observed x-ray intensities were far more intense than expected. The detailed mechanisms for x-ray emission from comets are still under hot discussion. Among various models proposed to explain the observed x rays, the most likely is x-ray emission following electron capture of highly charged solar ions in collisions with neutral constituent particles evaporated in the coma or tail of the comet [8,9].

In some fusion research devices, SiC, having a high melting temperature with low *Z* elements, is a good candidate material for covering the plasma-facing inner walls of

vacuum systems [10]. Photons, particularly their spectra, emitted from Si ions in various ionization stages confined in such high-temperature plasmas provide important clues for the diagnosis of high temperature plasma features of fusion reactor categories, where C ions are completely ionized. Relevant cross sections of electron capture for Si^{q+} ions have been found [11,12].

On the other hand, Si ions are also among the most abundant ions in the solar system after C, N, and O ions [13]. Recent data for low-energy electron capture have been published for low charged Si^{q+} ($q=3-5$) ions for astrophysical interest (Ref. [14] and references therein). In some solar systems such as Jupiter, S ions also are expected to play a significant role, but few investigations have been performed so far [15]. So far, few investigations have been performed to determine the cross sections for x rays that originate in electron capture into slow, highly charged ions colliding with neutral atoms and molecules [16].

In most of the present work, we have observed K x rays produced in collisions of H-like $\text{Si}^{13+}(1s)$, $\text{S}^{15+}(1s)$, and $\text{Ar}^{17+}(1s)$ ions, instead of bare Si^{14+} , S^{16+} , and Ar^{18+} ions, colliding with various gas targets including rare-gas atoms and molecules at relatively low energies (1–70 keV/u). There are two reasons for this choice. The first is due to the fact that more ion beams can be provided from the KSU EBIS ion source, compared with bare ions. The second is because it is easy to differentiate them from the commonly present impurity ions such as H_2^+ , C^{6+} , and O^{8+} ions with a same mass-charge ratio equal to 2. [During the course of the present work, we have found in the EBIS that this differentiation is, in principle, possible because heavier bare ions tend to have lower kinetic energy ($\sim 0.5\%$) due to trapping deep inside the electron space charge potential, compared with light ion impurity ions.] Some additional observations of x-ray spectra also have been performed for Si^{14+} ion impact, though its current could not be measured accurately and thus no cross sections could be determined.

EXPERIMENTAL SETUP AND PROCEDURES

H-like Si^{13+} , S^{15+} , and Ar^{17+} ions of about 10 pA are produced in the KSU EBIS through feeding of SiH_4 , H_2S , and Ar gases. They are first extracted at 4 kV from the EBIS and charge analyzed and, then, either accelerated up to 150 kV or decelerated down to about 2 kV. After passing a switching magnet and various steering-focusing lens systems, they are sent into a differentially pumped collision chamber containing target gas and then arrive at a Faraday cup. The ion current at the Faraday cup is integrated to obtain the total number of the incident ions and subsequently the cross sections. The inner surfaces of the collision chamber are carefully coated with carbon-containing aquadaq to avoid intense x rays from its aluminum wall which is impinged by the scattered projectile ions.

The x rays are observed with a Si Li detector with a 0.0125-mm Be window, which is energy calibrated with $K\alpha$ and $K\beta$ x rays from ^{55}Mn and also Si K and Ar K x rays emitted in photoionization. Its energy resolution is measured to be about 200 eV for 5.9-keV x rays. The x-ray counting

rates are kept to about 50 counts per second using a series of beam attenuators placed in the ion-beam path. Following the manufacturer's data sheet, the observed x-ray yields are corrected for the Be window transmission (estimated to be 82% for Si $K\alpha$, 90% for S $K\alpha$, and 98% for Ar $K\alpha$ x rays from these ions).

The linear increase of x-ray yields is confirmed when the gas pressure of the target chamber increases, as measured with a Baratron vacuum gauge. It also has been checked that the x-ray spectrum does not change when the target gas pressure changes. Absolute x-ray emission cross sections are determined through normalization to known Ar K x ray production cross section in 150-kV proton impact [17].

Uncertainties of the measured relative cross sections are estimated to be $\pm 20\%$, which originates mostly from the instabilities of the current integrator at low ion current ranges used in the present work and of low target gas pressure measurements. In addition, 15% uncertainties should be added to absolute cross sections due to those of the original Ar K x ray production in proton-Ar collisions [17].

RESULTS

A. Observed x-ray spectrum

Typical x-ray spectra emitted from low-energy 0.91-keV/u Si^{13+} , 0.92-keV/u S^{15+} , and 1.33-keV/u Ar^{17+} ions in collisions with neutral gas targets are shown in Fig. 1. In these ions, peaks due to $K\alpha$ as well as $K\beta, K\gamma, \dots$ x rays corresponding to $1snp \rightarrow 1s^2$ transitions resulting from one-electron capture into H-like ions are clearly observed: the latter $K\beta$ and $K\gamma, \dots$ x rays are inseparable due to the limited energy resolution of the present detector. Hereafter, we represent the sum of these $K\beta$ and $K\gamma, \dots$ peak intensities as simply $I(K\beta)$. Furthermore, in S^{15+} and Ar^{17+} ions, their L x rays also are observed, though they are strongly attenuated in the Be window (in addition to Al K x rays from the chamber wall). On the other hand, in Si^{13+} ion collisions, L x rays are almost completely absorbed in the Be window, and thus no trace of them is seen in the spectrum. The energies of $K\alpha$ x rays observed in collisions of Si^{13+} , S^{15+} , and Ar^{17+} ions are found to be 1.88, 2.44, and 3.18 keV (see Table I), which is in reasonable agreement with a simple expectation for transitions ($1snl \rightarrow 1s^2$) of He-like ions. The energies of these $K\alpha$ and $K\beta$ peaks are found to be the same for all the target gases studied within the energy resolution limit of the present detector. It is noted that there are slight changes of $K\beta/K\alpha$ intensity ratios, depending on target gases, suggesting that the electron is captured initially into different (nl) states for different targets, resulting in different cascade down to lower n states. Also, these $K\beta/K\alpha$ intensity ratios have been found to change when the collision energy is varied (see discussion that follows).

B. $K\beta/K\alpha$ intensity ratios

It is noted that the intensity ratios of $K\beta$ line to $K\alpha$ line, $I(K\beta)/I(K\alpha)$, emitted from these ions varied when the target gas or ion energy is changed. In the following these two features are discussed in detail.

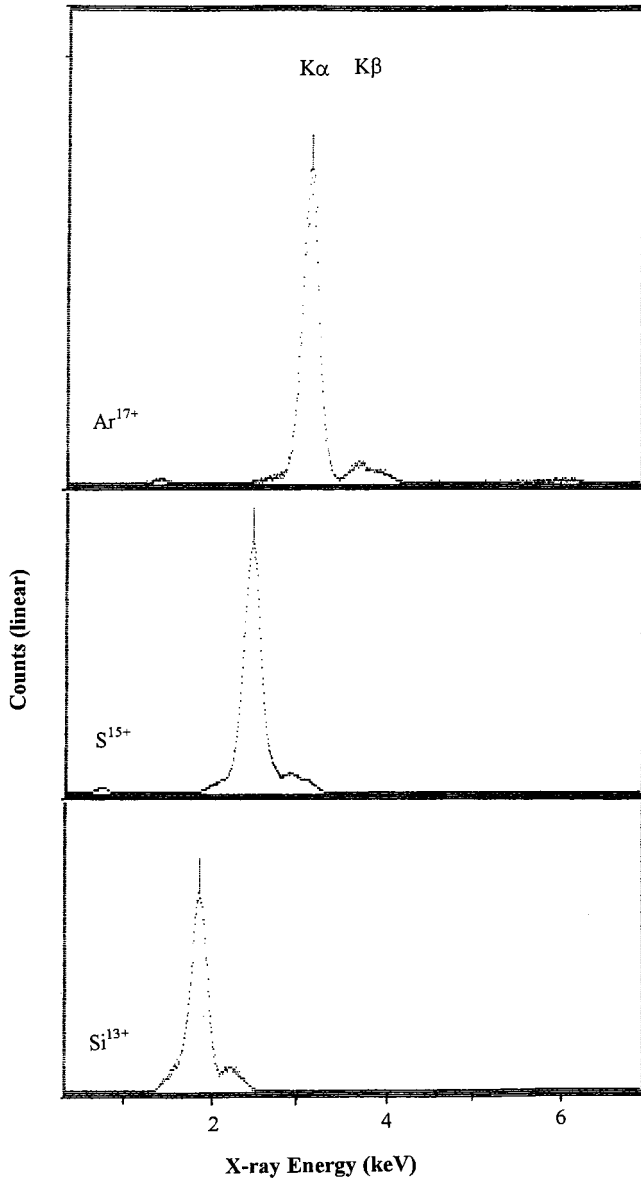


FIG. 1. Typical x-ray spectra from low-energy 0.91-keV/u Si^{13+} , 0.92-keV/u S^{15+} , and 1.33-keV/u Ar^{17+} ions colliding with neutral gas targets. Note that the peak energies move toward higher energies as the atomic number of ion increases from Si to Ar. Low-energy tails just below $K\alpha$ peaks are believed to be due to incomplete collection caused by the detector defect.

TABLE I. The observed $K\alpha$ and $K\beta$ x-ray energies (in units of keV) emitted from a H-like ion which captures an electron from neutral gas targets.

Ion	$K\alpha$ transition		$K\beta$ transition	
	Observed	Calculated	Observed	Calculated
Si^{13+}	1.88	1.91	2.23	2.27
S^{15+}	2.44	2.51	2.89	2.98
Ar^{17+}	3.18	3.20	3.77	3.79

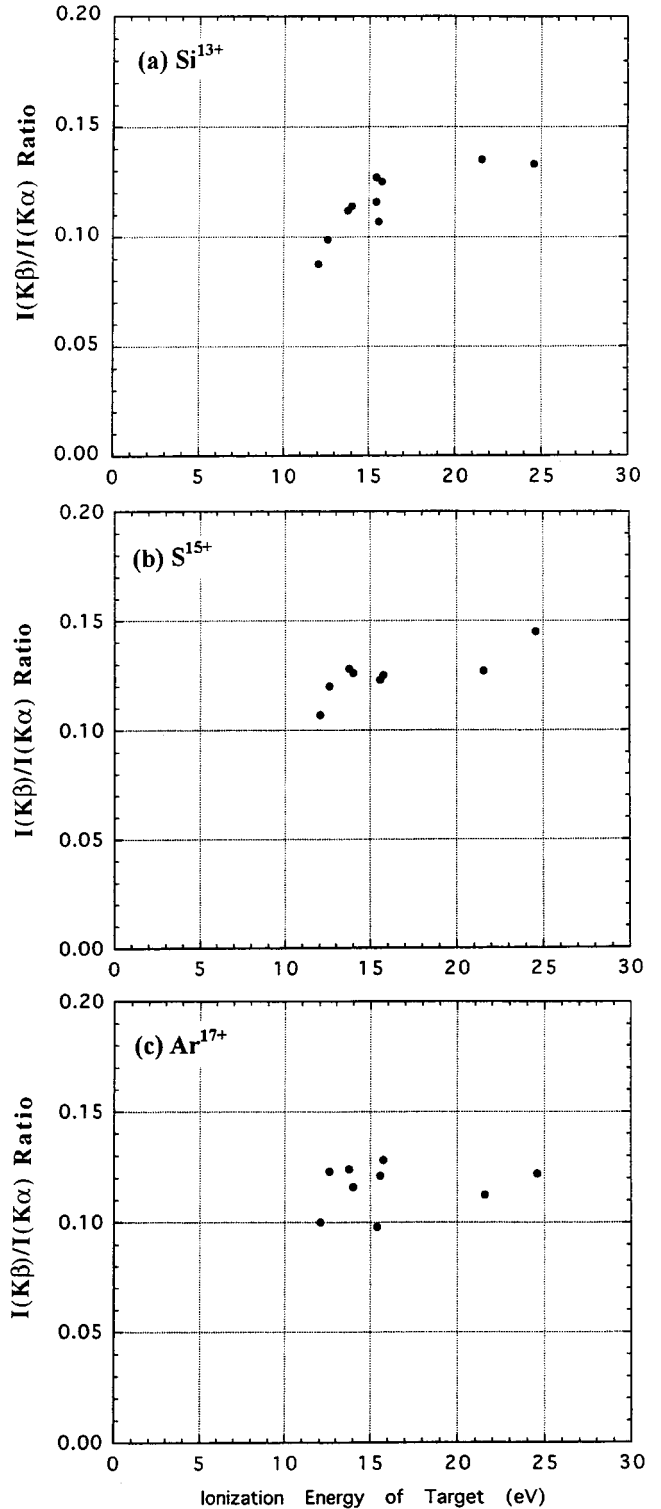


FIG. 2. Intensity ratios of the $K\beta$ line to the $K\alpha$ line, $I(K\beta)/I(K\alpha)$, observed in 0.91-keV/u (a) Si^{13+} , (b) 0.92-keV/u S^{15+} , and (c) 1.22-keV/u Ar^{17+} ion collisions as a function of the ionization energy of targets

1. Dependence on ionization energy of targets

As shown in Fig. 2, $I(K\beta)/I(K\alpha)$ ratios observed in 0.91-keV/u Si^{13+} ion collisions are found to be roughly of the order of 0.12, and to vary when the targets have been

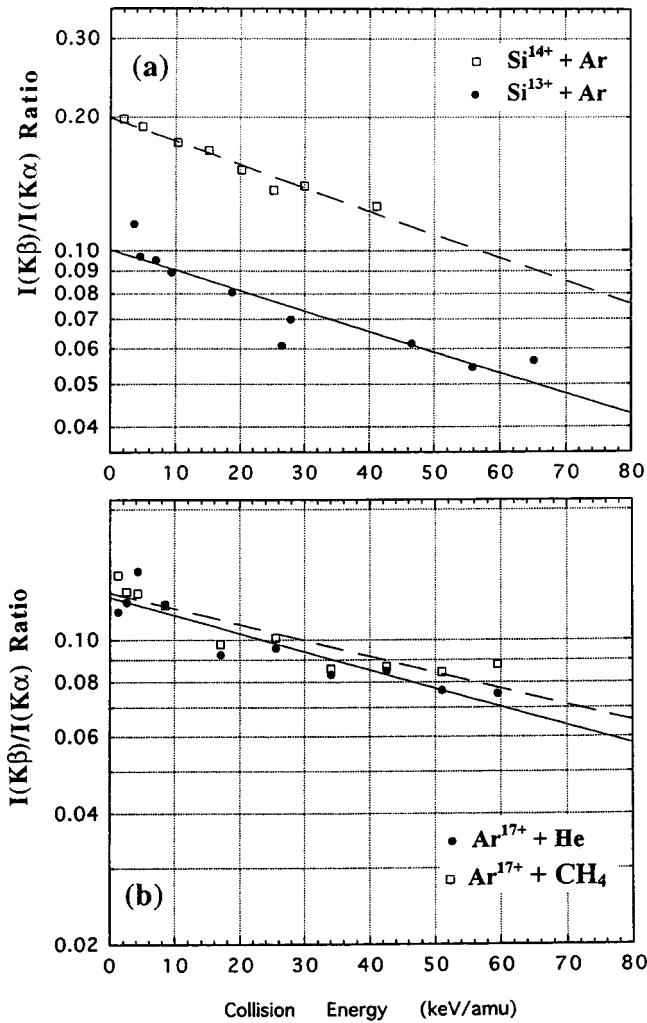


FIG. 3. Intensity ratios of the $K\beta$ line to the $K\alpha$ line, $I(K\beta)/I(K\alpha)$, ratios observed in (a) Si^{13+} and Si^{14+} ion collisions with Ar targets, and (b) Ar^{17+} ion collisions with He and CH_4 targets as functions of collision energy.

changed. In fact, $I(K\beta)/I(K\alpha)$ ratios increase when the ionization energy (I_b) of target gas increases, tending to be saturated at higher ionization energy. This indicates that, for different targets, the electron is captured into different (nl) states, depending on their ionization energy, and, in turn, cascades down differently. This can easily be understood to be due to the fact that the principal quantum number (n) of electron captured states becomes larger for target with low ionization energy [see Eq. (1)]. For example, based upon the classical-over barrier model, the electron is captured most likely to $n_0=5$ of Si^{13+} ions for He target atoms; meanwhile, $n_0=14$ for O_2 molecules, which is the lowest ionization energy used in the present work. Similar features also are seen for S^{15+} and Ar^{17+} ions, as shown in Figs. 2(b) and 2(c).

2. Dependence on collision energy

$I(K\beta)/I(K\alpha)$ ratios from Si^{13+} and also Si^{14+} for Ar, as shown in Fig. 3(a), are found to decrease when the ion impact energy increases. This is easily understood to be due to the longer time of higher excited states required to cascade

down to the lower states, and, thus, some fraction of them cannot emit x rays within a limited viewing zone of the detector. Similar features are seen for Ar^{17+} ions in He and CH_4 targets, as shown in Fig. 3(b). For the electron captured into higher excited states, as their lifetimes become longer, more time is required to come down to the lowest excited $2p$ and $3p$ states before emitting K x rays.

From the observed decrease of $I(K\beta)/I(K\alpha)$ ratios as a function of the collision velocity of the projectile ions, we can estimate the averaged lifetime (in fact their lifetime difference) of these states of ions. It has been found that the average lifetime difference is 6–7 ns, and varies slightly with target species and ions. This may be caused by the fact that through a larger number of cascades from higher n states for larger charge ions [see Eq. (1)], the (nl) distributions of electrons become statistically equilibrated and thus the initial features among the targets is lost.

C. Dependence of total cross sections on collision energy

It is known that the electron capture cross sections for highly charged ions ($q>5-6$) are roughly constant at low collision energy regions, and then slowly decrease as the ion collision energy increases. At higher energies, they decrease rapidly. Such a feature is one of the most common of electron-capture processes for highly charged ion-atom collisions [2]. The collision energy (1–70 keV/ u) dependences of the observed total x-ray emission cross sections resulting from Si^{13+} colliding with He and Ar targets are shown in Fig. 4(a). Indeed the observed cross sections are found to be roughly constant at low energies, and then decrease only slightly over the limited collision energy range investigated in the present work. These constant cross sections at lower energies are used in the following discussion. On the other hand, those for Ar^{17+} ions are nearly constant over the present collision energy (roughly 1–60 keV/ u), as shown in Fig. 4(b). This can be understood from the fact that the electron-capture cross sections can be expressed universally using the energy (keV/ u) divided by the ion charge as the energy scale [18].

D. Dependence of total cross sections on target ionization energy

On the other hand, the cross sections of electron capture decrease for targets with a high ionization energy and were empirically found to be roughly proportional to the inverse square of the ionization potential of targets [19–21]. This is understood classically to be due to the increase of the radius of the electron orbit when the ionization energy of the target decreases [22]. The observed dependence of total x-ray production cross sections for 0.91-keV/ u Si^{13+} ions colliding with various neutral targets is shown in Fig. 5(a) as a function of the inverse square of the ionization energy of targets. Indeed, the cross sections are shown to increase roughly linearly as the inverse square of the ionization potential, though there is scattering of some of the data. This simple relation can be used to estimate the cross sections that have not been measured so far or those for targets too hard to measure, such

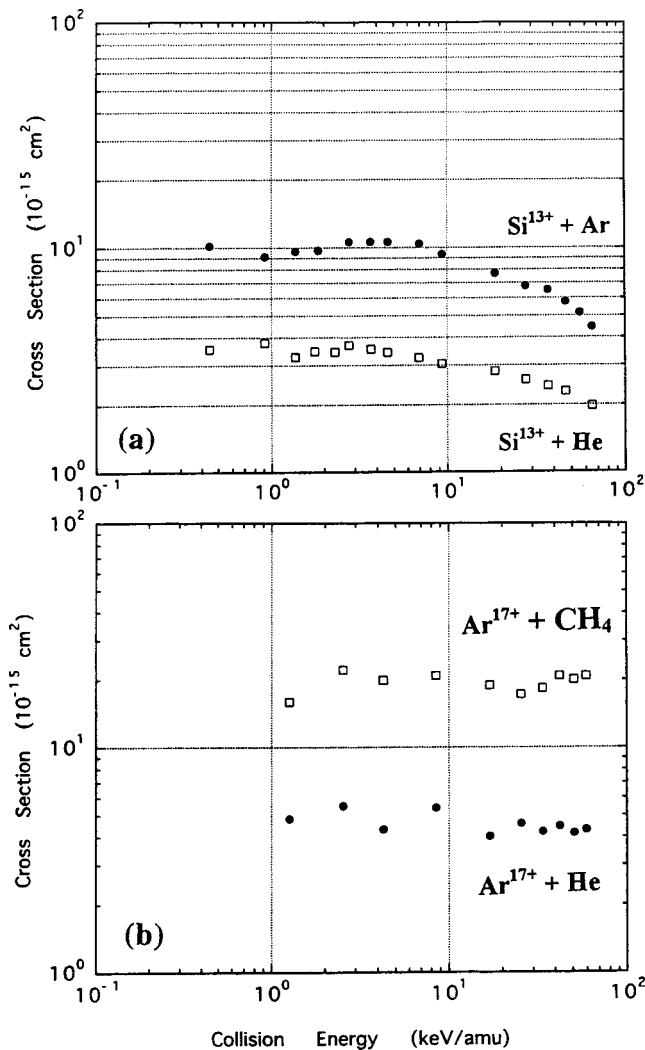


FIG. 4. K x-ray emission cross sections resulting from one-electron capture into (a) Si^{13+} from He and Ar targets and (b) Ar^{17+} from He and CH_4 targets.

as water vapor or metallic atom vapors. Similar results have been obtained for S^{15+} [Fig. 5(b)] and Ar^{17+} ions [Fig. 5(c)].

DISCUSSION AND SUMMARIES

It was already established that, in few-electron light target atoms such as He and H_2 , one-electron capture is dominant, and probabilities of multiple electron capture are small (at most 1–2% of total cross sections) [23,24]. On the other hand, for multielectron targets such as Ar and other molecules investigated here, multiple electron capture is known to contribute significantly to total electron-capture cross sections [25,26]. For example, 20–30% of total electron-capture cross sections can be due to double- and triple-electron capture in Ar targets over the present ion charge range. Then the cross sections for three-electron capture or greater are known to decrease quickly as the number of electrons captured increases.

Electrons are also known to be captured into highly excited states and, thus, most of the multiple electron capture forms so-called autoionization states that result in the emis-

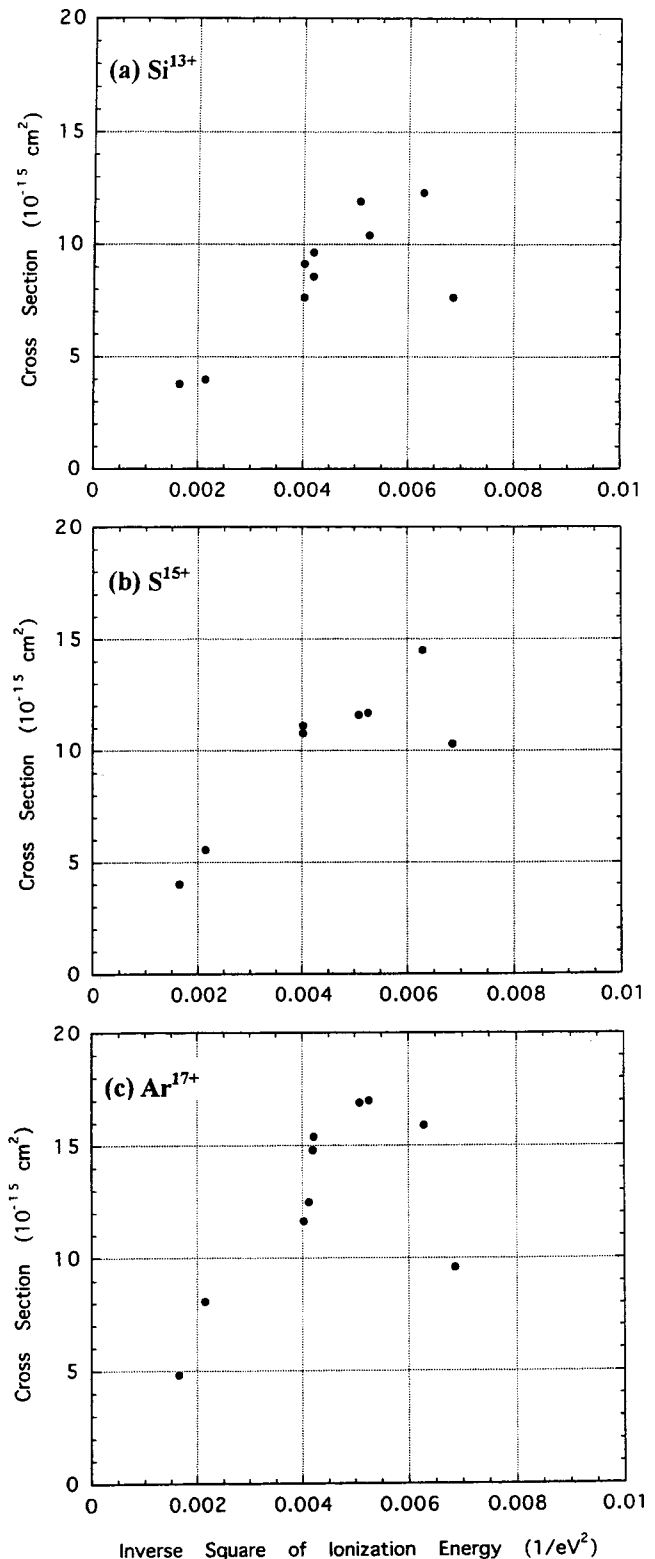


FIG. 5. X-ray emission cross sections at (a) 0.91-keV/ u Si^{13+} ions, (b) 0.92-keV/ u S^{15+} ions, and 1.33-keV/ u Ar^{17+} ions colliding with various atoms and molecules as functions of the inverse square of the ionization energy of targets.

sion of at least one electron and sometimes more electrons during a series of cascading de-excitation processes [27]. In the present ion charge range, only a few percent of two

TABLE II. Intensity ratios of $K\beta$ line to $K\alpha$ line, $I(K\beta)/I(K\alpha)$, emitted from H-like Si^{13+} , S^{15+} , and Ar^{17+} ions after electron capture collisions with neutral targets. The ratios for neutral Si, S, and Ar atoms are marked with asterisk (*) (Salem *et al.*).

$I(K\beta)/I(K\alpha)$ Ratios			
Si^{13+}	0.110	Si	0.027*
Si^{13+}	0.129	S	0.059*
Ar^{17+}	0.118	Ar	0.105*

electron-capture processes had been found to result in radiative emissions, suggesting that the dominant part of multi-electron capture goes to autoionization and emits one or more electrons [28–30]. At least one of the captured electrons goes down to $2p$ or $3p$ states, emitting K x rays. It can be assumed that all electron capture processes finally result in x-ray emission anyway, except for those formed in the metastable states. Therefore, K x ray emission cross sections would be expected to be related more closely with total electron capture cross sections than with one-electron capture cross sections.

On the other hand, though the cross sections for a number of one- or two-electron capture processes have been reported [2], few cross sections of total electron capture have been measured for these highly charged ions involving various atoms and molecules. Based upon the classical overbarrier model [22], total electron-capture cross sections can be related with the ionization energy I_b of the target and various empirical formulas already have been proposed to obtain total electron-capture cross sections. According to this model, total cross sections are proportional to the inverse square of the ionization energy of the target [20],

$$\sigma_t = 2.6(q/I_b^2) \quad (10^{-13} \text{ cm}^2), \quad (5)$$

where q is the initial charge of the primary ion, and I_b the first ionization energy of the target (in units of eV). This and similar empirical formulas [19,21] have been confirmed to reproduce quite nicely the observed data for rare gas atoms over a wide range of parameters (q, I_b) [15,24–26,30–34].

As shown above in Fig. 5, it is noted that there is some scattering that may be due to special features of target gases. For example, the x-ray production cross sections for O_2 are always smaller than those having similar ionization energy. Probably this can be related to the fact that O_2 molecules are highly electronegative, compared with others studied here and thus tend to keep their electrons or take back electrons which form the electron cloud of the quasimolecule during collisions. But the observed x-ray cross sections are, roughly speaking, found to be proportional to the inverse square of the ionization energy of targets for all ions investigated here (Si^{13+} , S^{15+} , and Ar^{17+}).

Though there are slight variations of intensity ratios, $I(K\beta)/I(K\alpha)$, depending on the kind of targets, as shown in Fig. 2, we also can take some average over all of them, as shown in Table II. It is interesting to note that the measured $I(K\beta)/I(K\alpha)$ ratios for these H-like ions averaged over all

the neutral gas targets used in the present work are quite large, compared with those for neutral atoms, in particular for lower Z ions. In fact, though the ratios for neutral targets increase as the Z increases [35], depending strongly on the outer-shell electron configurations (particularly for $K\beta$ transitions), they seem to be roughly constant for all of these highly charged ions investigated here. This feature seems to be quite reasonable as the electron is captured to highly excited states ($n \geq 5$ in most of the present cases) of ions with one K -shell vacancy and needs a number of cascades down before reaching the $2p$ or $3p$ state. A series of such cascade processes (at least relative branching ratios) for He-like ions tends to make $I(K\beta)/I(K\alpha)$ ratios almost insensitive to their atomic number as far as the electron is captured into very highly excited states.

It is also important to know a relationship between electron capture cross sections and K x-ray emission cross sections in highly charged ion collisions. As mentioned already, K x-ray emissions from low energy, bare, and H-like ion collisions are closely related with electron-capture processes. As an electron is always captured at higher n_0 states during highly charged ion-neutral target collisions [see Eq. (1)], it is theoretically and experimentally understood that probabilities of direct decay from such highly excited ($n_0 l_0$) states to the ground state, namely, $1s n_0 p \rightarrow 1s^2$ state transitions, is very small but a series of cascade-down processes is dominant [see processes (3) and (4) above].

There are a number of measurements of electron-capture cross sections for some targets used here such as rare-gas atoms. Generally they covered only a limited range of collision energy. In particular they are very scarce for molecular targets, except for molecular hydrogen. There are some reasons for this situation. This is probably due to the fact that such investigations involving highly charged ions are more or less intended to be used for fusion applications where practically no molecules, except for hydrogen molecules, exist. Recently a strong interest in highly charged ions in collisions with molecules was raised in applications to astrophysics, as mentioned in the Introduction [6]. Fortunately we have relatively simple but reasonably reliable empirical formulas to estimate total electron-capture cross sections to within about 20% uncertainties. Though this empirical formula has not been tested fully for molecular targets, it has been found that the existing electron-capture cross sections for molecular hydrogen and simple molecules are in agreement with this scaling [36]. This can be expected to be valid for other molecular targets, too.

In the present work, we have shown that x-ray production cross sections are roughly proportional to the inverse square of the ionization energy of targets including a number of molecules, as seen in Fig. 5. To our knowledge this is the first time such a trend is shown in x-ray production involving highly ionized ions. This empirical knowledge is quite convenient for estimating cross sections for other targets.

As mentioned already, electrons captured into highly excited states of highly charged ions are more likely to cascade down, instead of by direct transitions to the ground state, before complete stabilization. After electron capture and the following cascading processes, some fraction of highly

TABLE III. A list of the measured x-ray production cross sections and their ratios over total (empirical) electron capture cross sections [see Eq. (5)] for ~ 1 -keV/ u ions with $q=13+$, $15+$, and $17+$ colliding with various target gases (in units of 10^{-15} cm²). I_b is the ionization energy of the target (in eV).

Target	I_b (eV)	X-ray cross section (10^{-15} cm ²)			X-ray total electron capture			Comments
		Ar ¹⁷⁺	S ¹⁵⁺	Si ¹³⁺	Ar ¹⁷⁺	S ¹⁵⁺	Si ¹³⁺	
He	24.59	4.81	4.01	3.79	0.659	0.622	0.679	
Ne	21.56	8.07	5.56	3.99	0.849	0.663	0.549	
Ar	15.76	11.6	10.8	9.14	0.654	0.687	0.672	
N ₂	15.58	12.4	11.1	7.64	0.686	0.691	0.549	
H ₂	15.43	14.8	9.55	9.64	0.796	0.582	0.679	
D ₂	15.43	15.4	11.6	8.57	0.826	0.665	0.604	
CO	14.01	16.9	11.6	11.9	0.751	0.583	0.691	
CO ₂	13.77	17.0	11.7	10.4	0.730	0.568	0.583	
CH ₄	12.61	15.9	14.5	12.3	0.572	0.592	0.579	
O ₂	12.07	9.59	10.3	7.64	0.317	0.340	0.329	

charged ions ends up in the metastable states such as in the $1s2s$ states. Note that the metastable ($1s2s\ 2^3S_1$) state decays only via the quadrupole magnetic transition, emitting two photons with continuous energy distributions. The lifetimes in the present ion range are a few hundred ns, which are so long that photons cannot be emitted within a limited detector viewing zone. Similarly, the metastable ($1s2s\ 2^1S_0$) state He-like ion decays only via the two-photon electric dipole transition, emitting two x-ray photons with continuous energy distributions and thus no K x-ray peak from this decay can be observed with a single detector [37]. Note that, as the metastable ions in the present ion range ($Z=14-18$) have lifetimes of a few 10 ns [38], most of the metastable state ions at low collision energies decay within a viewing zone of the x-ray detector.

It would be important to know what fractions of the captured electrons come down to the metastable states, and cannot emit K x rays within the viewing zone. A comparison between total electron capture cross sections and K x-ray emission cross sections may provide important information to this question. So far some detailed understanding of electron-capture processes has been obtained, and data for electron-capture cross sections are available [2]. But data for bare or H-like ions are still not sufficient. In particular, there are no systematic measurements for molecular targets yet, as noted above. In Table III we give a summary of both the present x-ray emission cross sections and their ratios to total electron-capture cross sections. Those shown for electron capture are calculated values based upon the empirical formula [Eq. (5)]. Though some data are scattered, the average ratio for K x-ray emission cross sections to total electron capture cross sections is found to be $\sim 0.62 \pm 0.08$ (0.66 excluding O₂ data), indicating that, on average, 38% (34%) of ions having electrons captured are tentatively stabilized into the metastable states without emitting K x rays. Under the assumption that the (nl) distributions are nearly statistically populated after a series of cascading processes from highly excited capture states, the fraction of ions reaching the $2s$ metastable state is estimated to be $1/3$, with the remaining two-thirds going down to the $1s$ ground state by emitting K

x rays. Though these ratios strongly depend on various atomic parameters such as transition probabilities, branching ratios, etc., no detailed theoretical analysis or models have been proposed to know what fractions of the electron captured ions emit K x rays [39].

This fraction also can be interesting when compared with those obtained in high energy (MeV/ u) experiments. Fractions of the ($1s2s$) metastable states in He-like F⁷⁺ and Si¹²⁺ ions produced when passing through thin stripping foils have been determined, with the enhancement of target x-ray production, as a function of collision energy [39,40]. It was found experimentally that the fractions increased rapidly as the collision energy increased at the low collision energy region and their maximum fractions reached $\sim 30\%$ of total He-like ions at around the incident ion velocity, roughly equal to the orbital velocity of the $1s$ electron, where this electron easily can be excited to higher states or ionized to the continuum. So far there is no clear quantitative understanding why such large fractions of the metastable state ions can be formed. At low collision energies, the $1s$ electron of the incident particle cannot be ionized or excited but, as the collision energy increases, production of such highly ionized or excited state ions becomes significant. In fact, through continuous collisions inside foils, one of the $1s$ electrons in high energy incident ions is successively excited to high n -states ($1s^2 \rightarrow 1snl \rightarrow 1sn'l' \dots$ for He-like ions) and finally the (nl) distributions are equilibrated. Upon leaving the final surface of foils, the electrons in a highly excited state start to cascade down to the ground state with some going to the metastable state (There are also some chances for the $1s$ electron to be ionized and, in the succeeding collisions, another electron can be captured into highly excited states, which are stabilized after leaving the foil.) This can explain the observed high fraction of the metastable state ions at sufficiently high collision energies.

This comparison between the observed fractions of the metastable state ions strongly suggests that, both at low and high energies, the metastable ($1s2s$) state ions are formed through a similar or practically the same mechanism, namely,

either excitation to highly excited states (for high energy ions) or electron capture into highly excited states (for low energy, highly charged ions), which is followed by cascading down to $2s$ states. This sequence can explain the fact that the observed fractions of the metastable state ions are unexpectedly high and practically the same both for low energy H-like ions where electron capture is dominant and for high-energy ions that are formed through successive collisions in solids.

ACKNOWLEDGMENTS

The present authors would like to thank C. W. Fehrenbach and Paul Gibson for providing various ion beams used in the present experiment. This work was supported by the Chemical Sciences, Geosciences and Biosciences Division, Office of Basic Energy Science, Office of Science, U.S. Department of Energy. P. C. S. acknowledges support from NASA Grant No. NAG5 9088.

-
- [1] R.K. Janev and H. Winter, *Phys. Rep.* **117**, 265 (1985).
 [2] R. K. Janev, L. P. Presnyakov, and V. P. Shevelko, *Physics of Highly Charged Ions* (Springer, Berlin, 1985).
 [3] H. Ryufuku, K. Sasaki, and T. Watanabe, *Phys. Rev. A* **21**, 745 (1980).
 [4] R.E. Olson, *Phys. Rev. A* **24**, 1726 (1981).
 [5] R. Mann, F. Folkmann, and H.F. Beyer, *J. Phys. B* **14**, 1161 (1981).
 [6] C. M. Lisse, K. Dennerl, J. Enghauser, M. Hayden, F. E. Marshall, M.J. Mumma, R. Petre, P. Pye, M.J. Ricketts, J. Schmitt, J. Trümper, and R. G. West, *Science* **274**, 205 (1996).
 [7] M. J. Mumma, V. A. Krasnopolsky, and M. J. Abbott, *Astrophys. J.* **481**, L125 (1997).
 [8] T. E. Cravens, *Astrophys. J.* **532**, L153 (2000).
 [9] V. Kharchenko and A. Dalgarno, *J. Geophys. Res.* **105**, 1851 (2000).
 [10] *Atomic and Molecular Data for Fusion*, edited by H.W. Drawin and K. Katsonis, special issue of *Phys. Scr.* **23** (1980).
 [11] W. Fritsch and H. Tawara, *Nucl. Fusion* **30**, 373 (1990).
 [12] C. Cisneros, J. de Uguijo, I. Alvarez, A. Aguilar, A. M. Juarez, and H. Martinez, *Suppl. Nucl. Fusion* **6**, 247 (1995).
 [13] P. Bochsler, *Phys. Scr.* **T18**, 55 (1987).
 [14] H. Tawara, K. Okuno, C. W. Fehrenbach, C. Verzani, M. P. Stockli, B. D. Depaola, P. Richard, and P. C. Stancil, *Phys. Rev. A* **63**, 062715 (2001), and references therein.
 [15] T. Iwai, Y. Kaneko, M. Kimura, N. Kobayashi, A. Matsumoto, S. Ohtani, K. Okuno, S. Takagi, H. Tawara, and S. Tsurubuchi, *J. Phys. B* **17**, L95 (1984).
 [16] J. B. Greenwood, I. D. William, S. J. Smith, and A. Chutjian, *Astrophys. J.* **533**, L175 (2000).
 [17] K. G. Harrison, H. Tawara, and F. J. de Heer, *Physica (Amsterdam)* **66**, 16 (1973).
 [18] H. Ryufuku and T. Watanabe, *Phys. Rev. A* **20**, 1828 (1979).
 [19] A. Müller and E. Salzborn, *Phys. Lett.* **62A**, 329 (1977).
 [20] M. Kimura, N. Nakamura, H. Watanabe, I. Yamada, A. Danjo, K. Hosaka, A. Matsumoto, S. Ohtani, H. A. Sakaue, M. Sakurai, H. Tawara, and M. Yoshino, *J. Phys. B* **28**, L643 (1995).
 [21] N. Selberg, C. Biedermann, and H. Cederquist, *Phys. Rev. A* **54**, 4127 (1996).
 [22] A. Niehaus, *J. Phys. B* **19**, 2925 (1986).
 [23] V. P. Shevelko and H. Tawara, *Atomic Multielectron Processes* (Springer-Verlag, Berlin, 1998).
 [24] J. Vancura, V. J. Marchetti, J. J. Perotti, and V. O. Kostroun, *Phys. Rev. A* **47**, 3758 (1993).
 [25] J. Vancura, J. S. Perotti, J. Flidr, and V. O. Kostroun, *Phys. Rev. A* **48**, 2515 (1994).
 [26] R. Ali, C. L. Cocke, M. L. Raphaelian, and M. P. Stockli, *Phys. Rev. A* **49**, 3586 (1994).
 [27] M. Barat and P. Roncin, *J. Phys. B* **25**, 2205 (1992).
 [28] H. Cederquist, H. A. Andersen, E. Beebe, C. Biedermann, L. Broström, Å. Enström, H. Gao, R. Hutton, J. C. Levin, L. Liljeby, M. Pajek, T. Quinteros, N. Selberg, and P. Sigray, *Phys. Rev. A* **46**, 2592 (1992).
 [29] F. Krok, I. Yu. Tolstikhina, H. A. Sakaue, I. Yamada, K. Hosaka, M. Kimura, N. Nakamura, S. Ohtani, and H. Tawara, *Phys. Rev. A* **56**, 4792 (1997).
 [30] N. Nakamura, F. J. Currel, A. Danjo, M. Kimura, A. Matsumoto, S. Ohtani, H. Sakaue, M. Sakurai, H. Tawara, H. Watanabe, I. Yamada, and M. Yoshino, *J. Phys. B* **28**, 2959 (1995).
 [31] R. Mann, *Z. Phys. D: At., Mol. Clusters* **3**, 85 (1986).
 [32] H. Tawara, T. Iwai, Y. Kaneko, M. Kimura, N. Kobayashi, A. Matsumoto, S. Ohtani, K. Okuno, S. Takagi, and S. Tsurubuchi, *J. Phys. B* **18**, 337 (1985).
 [33] P. Hvelplund, A. Barany, H. Cederquist, and J. O. K. Pedersen, *J. Phys. B* **20**, 2515 (1987).
 [34] H. Andersen, G. Astner, and H. Cederquist, *J. Phys. B* **21**, L187 (1988).
 [35] S.I. Salem, S.L. Panossian, and R.A. Krause, *At. Data Nucl. Data Tables* **14**, 91 (1974).
 [36] K. Hosaka, H. Tawara, I. Yamada, H. A. Sakaue, F. Krok, F. J. Currel, N. Nakamura, S. Ohtani, H. Watanabe, A. Danjo, M. Kimura, A. Matsumoto, M. Sakurai, and M. Yoshino, *Phys. Scr.* **T73**, 273 (1997).
 [37] R. Marrus and P.J. Mohr, *Adv. At. Mol. Phys.* **14**, 181 (1978).
 [38] D.W. Drake and A. van Wijngaarden, *Physics of Highly-Ionized Atoms*, Vol. 20 of *NATO Advanced Study Institute, Series B: Physics*, edited by R. Marrus (Springer-Verlag, Berlin, 1989), p. 143.
 [39] U. Schiebel, B.L. Doyle, J.R. Macdonald, and L.D. Ellsworth, *Phys. Rev. A* **16**, 1089 (1977).
 [40] M. Terasawa, T. J. Gray, S. Hagmann, J. Hall, J. Newcomb, P. Pepmiller, and P. Richard, *Phys. Rev. A* **27**, 2866 (1983).